

# Hybrid TOA/AOA Virtual Station Localization Based on Scattering Signal Identification for GNSS-Denied Urban or Indoor NLOS Environments

Rui Luo <sup>1</sup>, Lili Yan <sup>2</sup>, Ping Deng <sup>2,\*</sup> and Yin Kuang <sup>1</sup>

<sup>1</sup> Key Laboratory of Interior Layout optimization and Security, Chengdu Normal University, Chengdu 611130, China

<sup>2</sup> Key Laboratory of Information Coding and Transmission, Southwest Jiaotong University, Chengdu 611756, China

\* Correspondence: pdeng@swjtu.edu.cn

**Abstract:** Accurate localization is the premise of many technologies and applications, such as navigation, emergency assistance and wireless sensor network. For Global Navigation Satellite System (GNSS)-denied urban or indoor environments, various localization technologies based on mobile communication networks or other wireless technologies have been designed and developed. The main challenge for these localization technologies is the presence of a non-line-of-sight (NLOS) propagation environment due to dense obstacles or buildings. The virtual station method is a promising high-accuracy target localization technique in NLOS environments, and the localization of the scatterer is key to the virtual station method. Once one-bounce scattering signals from the same scatterer are identified, the localization of the scatterer can be achieved easily with the existing localization algorithm of line-of-sight (LOS) scenario, and then the localization of NLOS scenarios is converted into a problem of LOS easily. In this paper, a hybrid time of arrival (TOA)/angle of arrival (AOA) virtual station localization algorithm based on scattering signal identification is proposed. Firstly, one-bounce scattering signals from the same scatterer are identified based on TOA/AOA measurements. Next, scatterers are located based on one-bounce scattering signals with the LOS localization algorithm, and then scatterers are regarded as virtual stations and used for mobile station (MS) localization. Compared with the existing research on the virtual station method, the proposed algorithm relies only on TOA/AOA measurements and does not require any assumption or prior knowledge about the scatterer, base station (BS) or MS, which provides a solid foundation for feasible target localization. Simulation results demonstrate, as far as we know, the proposed algorithm outperforms the state-of-the-art hybrid TOA/AOA algorithm in localization accuracy.

**Keywords:** angle of arrival (AOA); localization; non-line-of-sight (NLOS); scattering signal; time of arrival (TOA); virtual station



**Citation:** Luo, R.; Yan, L.; Deng, P.; Kuang, Y. Hybrid TOA/AOA Virtual Station Localization Based on Scattering Signal Identification for GNSS-Denied Urban or Indoor NLOS Environments. *Appl. Sci.* **2022**, *12*, 12157. <https://doi.org/10.3390/app122312157>

Academic Editor: Qian Meng

Received: 6 November 2022

Accepted: 25 November 2022

Published: 28 November 2022

**Publisher's Note:** MDPI stays neutral with regard to jurisdictional claims in published maps and institutional affiliations.



**Copyright:** © 2022 by the authors. Licensee MDPI, Basel, Switzerland. This article is an open access article distributed under the terms and conditions of the Creative Commons Attribution (CC BY) license (<https://creativecommons.org/licenses/by/4.0/>).

## 1. Introduction

Target localization has a variety of applications, such as emergency assistance, people and asset tracking, location-based advertising or billing and intelligent transportation systems. GNSS provides high-accuracy real-time localization services in outdoor open-sky environments, but in GNSS-denied urban or indoor environments, accurate localization is still an unsolved problem due to the unavailability or degradation of GNSS signals. For GNSS-denied urban or indoor environments, various localization technologies based on mobile communication networks or other wireless technologies such as WiFi, Ultra-Wideband (UWB) has been designed and developed. For localization technologies based on mobile communication networks or other wireless technologies, measurements in the localization of MS typically include distance-based parameters such as TOA [1–5] and time-difference-of-arrival (TDOA) [6,7], received signal strength (RSS) [8,9], AOA [10] or

their combinations [11]. These algorithms are proved to be very effective for applying in open-air environments, in which the LOS signals are dominant. However, NLOS radio propagation between BS and MS generally exists in the localization scenarios, due to dense obstacles or buildings, which dramatically degrade the performance of localization algorithms. NLOS is considered the most severe source of positioning error [12]. NLOS propagation results in time and angle measurements error. For time-based localization systems, the extra propagation distance of the NLOS signal directly corresponds to an overestimate of the distance between the MS and BS, for direction-based localization systems, the angle from which the signal arrives at the MS is not in the true direction to the BS. This leads to severe degradation of localization accuracy if standard LOS localization estimation algorithms are employed.

To mitigate the NLOS impact, a variety of techniques and algorithms have been proposed in the literature. Conventional methods to process the NLOS effect can be mainly divided into three categories. One category identifies and discards NLOS signals so that only the LOS signal is applied for localization [13–15]. This can achieve proper localization performance if the NLOS signals are detected correctly and the number of remaining LOS links is sufficient for localization (e.g., three LOS links of distance measurements for 2D scenarios and four links for 3D scenarios). This type of solution would be problematic in scenarios, where the LOS signal is not available due to the effect of ray blocking. The other category tries to mitigate the negative impact of NLOS measurements and exploits both LOS and NLOS signals, such as the residual-based method [16–19] and NLOS propagation model compensation [20–25]. However, the residual-based method requires a sufficient number of LOS BSs for localization, which cannot be guaranteed in practical localization scenarios and NLOS propagation model compensation requires explicit knowledge of the NLOS propagation model or historical measurements, which has limitations in practical applications.

The third category is the virtual station method, which locates the scatterers in the NLOS environment first, and then uses scatterers as virtual stations, so the localization of NLOS scenarios is converted into a problem of LOS and the accuracy of localization can be improved greatly compared to other categories due to making full use of the additional information of the scatterers. Therefore, the virtual station method has received immense attention in the research society [26–32], owing to its great potential for development. The authors of [26] proposed a scattering distance-based (SDB) algorithm using TOA and AOA measurements from a single BS, which estimates iteratively the MS position by estimating the unknown scatterer positions in a prior step, but this algorithm only applies to the case of the ring-of-scatterers (ROS) model, and its performance depends on the accuracy of the initial estimate of the position of MS, which is determined by another localization algorithm in the NLOS environment. In [27], a maneuverable single station is introduced for the NLOS environment. With scatterers regarded as virtual observation stations, the problem of the single-station localization can be converted into a problem of multi-station localization. Whereas the maneuverable BS is an unrealistic assumption in practical scenarios usually, at the same time, this algorithm has high computational complexity or is sensitive to ranging errors. The authors of [28–30] proposed a geometrical approach to locating virtual stations for the NLOS environments and then located MS based on the positions of virtual stations. However, these algorithms need floor plan information and assume that all reflectors in the scenario are pure and have smooth and regular surfaces, which may be unavailable in practical environments. In [31], pedestrian dead reckoning (PDR) is adopted to construct the virtual station, then the LOS BS and virtual stations participate in the localization of MS with minimum residual. However, when the error of the initial position estimate of MS is large, the algorithm performance will dramatically degrade, meanwhile, PDR is indispensable for the construction of virtual stations, which might limit its applicability in many situations.

For any virtual station method, the localization of scatterers is key to the algorithm. On the other hand, as long as the one-bounce scattering signals from the same scatterer are

identified, the scatterer can be located accurately with existing LOS algorithms, and then the localization of NLOS scenarios is converted into a problem of LOS easily. Hence, the identification of one-bounce scattering signals from the same scatterer is key to the virtual station method in the NLOS environment. In this paper, we propose a hybrid TOA/AOA virtual station localization algorithm based on scattering signal identification for GNSS-denied urban or indoor NLOS environments. Our main contributions are as follows:

1. A two-step one-bounce scattering signal identification algorithm used for localization of scatterers is proposed, which does not require any assumption or prior knowledge about MS, BS and scatterer.
2. With scatterers regarded as virtual stations, a virtual station localization algorithm is proposed, which outperforms the state-of-the-art hybrid TOA/AOA algorithm in localization accuracy, as far as we know.

The remaining of this paper is organized as follows. In Section 2, the first step of the one-bounce scattering signal identification algorithm is described. The second step of the one-bounce scattering signal identification algorithm is presented in Section 3. Section 4 is devoted to the virtual station localization algorithm. Section 5 is simulations and performance analysis. Finally, conclusions are given in Section 6.

## 2. First Step of One-Bounce Scattering Signal Identification Algorithm

### 2.1. System Model

The system model assumes that direct signal is either obstructed or interfered with by multipath components, signals only propagate through the NLOS signals. Although the exact scattering environments should involve multiple-bounce scattering signals, one-bounce scattering is assumed because multiple-bounce scattering signals can be ignored as they suffer from severe attenuation and are almost negligible [32], which is well-fitted for modeling multipath propagation channels, especially in urban or indoor environments, this assumption is also made in the work of [33].

In one-bounce scattering environments, a signal is transmitted from the transmitter (MS) to the receiver (BS) via scatterer. For a simple scenario with one MS, two BSs and three scatterers, the geometric position relationship of BS, scatterer and MS, as well as one-bounce scattering signals are depicted in Figure 1. MS is located at T, S1, S2 and S3 are all one-bounce scatterers. A and B are BS. Suppose that BS A detects two one-bounce scattering signals from S1 and S2, path 2 and path 1, respectively. BS B detects two one-bounce scattering signals from S1 and S3, path 3 and path 4, respectively. In Figure 1, two one-bounce scattering signals from the same scatterer S1, path 2 and path 3, are detected by BS A and B, respectively. The scatterers like S1, whose scattering signals are detected by multiple BSs, will be located with our proposed algorithm and used as a virtual station for MS localization.

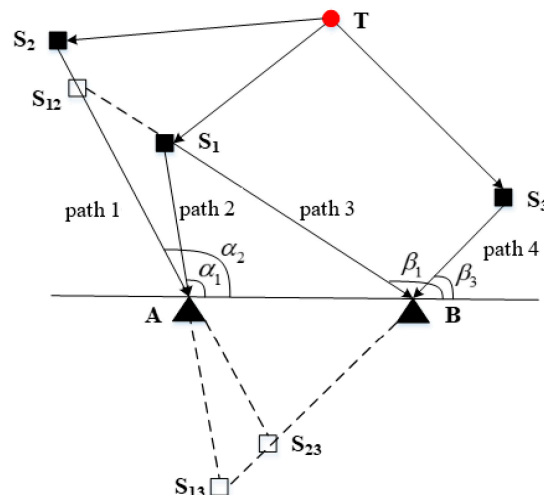


Figure 1. Geometry of one-bounce scattering system model.

### 2.2. Identification under Condition of Two BSs

First, consider a simple scenario with only two BSs as depicted in Figure 1. The coordinates of BS A and BS B are  $(x_A, y_A)$  and  $(x_B, y_B)$ , respectively. BS A detects two one-bounce scattering signals from S1 and S2, path 2 and path 1, their AOA is  $\alpha_1$  and  $\alpha_2$ , respectively. Corresponding to the two one-bounce scattering signals, the distance of TOA from MS to BS A is  $d_{TS_1A}$  and  $d_{TS_2A}$ , respectively. Similarly, BS B detects two one-bounce scattering signals from S1 and S3, path 3 and path 4, their AOA is  $\beta_1$  and  $\beta_2$ , the distance of TOA from MS to BS B is  $d_{TS_1B}$  and  $d_{TS_3B}$ , respectively.

For every pair scattering signal combination whose scattering signals are received by two different BSs, for instance, BS A and BS B, the two scattering signal lines intersect at a point, this point may be a scatterer. Suppose that the coordinate of the intersect point is  $(x_s, y_s)$ , based on AOA, coordinates of BS and intersect point, we can obtain a linear equation for every scattering signal line, accordingly, the two scattering signal lines satisfy linear equations as Equation (1):

$$\begin{cases} y_s - y_A = \tan\alpha_i(x_s - x_A) \\ y_s - y_B = \tan\beta_i(x_s - x_B) \end{cases} \quad i = 1, 2 \tag{1}$$

As depicted in Figure 1, for the four scattering signals that BS A or BS B receive, there are four pairs of scattering signal combination, and four intersection points accordingly, that is, S1, S13, S12 and S23, which are all potential scatterers from which emit two scattering signals arriving BS A and BS B, respectively, the four intersection points are all denoted as S.

It can be observed from Figure 1 that the intersection points of two scattering signal lines, that is, potential scatterers, can be divided into two categories: the real scatterer that emits two scattering signals arriving BS A and BS B, such as S1; the other just intersection point of two scattering signal lines, but not real scatterers, such as S13, S12 and S23. Obviously, for the identification of a one-bounce scattering signal from the same scatterer, the latter should be identified as a false scatterer, and the corresponding two scattering signals are not scattering signals from the same scatterer.

Based on Equation (1), we can get the coordinates of potential scatterers S, that is,  $(x_s, y_s)$ , so the distances between potential scatterer S and BS A, denoted by  $d_{SA}$ , can be computed. The distance between potential scatterers S and BS B, denoted by  $d_{SB}$ , is similar. As depicted in Figure 1, if the potential scatterer S is a real scatterer between MS and BS A, the TOA distance between MS and BS A, which is denoted by  $d_{TSA}$ , is the sum of the distance from MS to scatterer denoted by  $d_{TS}$  and distance from scatterer to BS A denoted by  $d_{SA}$ , so we can have

$$d_{TSA} = d_{TS} + d_{SA} \tag{2}$$

Similarly, for BS B, we have

$$d_{TSB} = d_{TS} + d_{SB}. \tag{3}$$

Hence,

$$d_{TSA} - d_{SA} = d_{TSB} - d_{SB} \tag{4}$$

Nevertheless, Equation (4) does not hold for a false scatterer. Therefore, the real scatterer can be distinguished from the false scatterer based on Equation (4). Considering the measurement error, the identification formula is expressed as:

$$||d_{TSA} - d_{SA}| - |d_{TSB} - d_{SB}|| < D, \tag{5}$$

where  $D$  is the identification threshold. Clearly, with increasing threshold value, a false scatterer is more likely to be identified as a real scatterer, however, a real scatterer is increasingly impossible to be identified as a false scatterer. We define false alarm probability as the probability that a false scatterer is identified as a real scatterer, and alarm dismissal probability is the probability that a real scatterer is identified as a false scatterer. With

increasing threshold value, the false alarm probability will increase and the alarm dismissal probability will decrease. Hence, the setting of identification threshold  $D$  depends on the trade-off between false alarm probability and alarm dismissal probability.

### 2.3. Identification under Condition of More than Two BSs

In practical environments, there are more than two BSs, suppose there are  $M$  BSs, the coordinate of the  $i$ th BS is  $(x_i, y_i)$ ,  $i = 1, 2, \dots, M$ , the coordinate of MS is  $(x, y)$  and scatterers distribute around the MS. Moreover, suppose that the  $M$  BSs receive  $N$  one-bounce scattering signals from multiple scatterers.

For the  $N$  one-bounce scattering signals, there are  $C_N^2$  pairs of scattering signal combinations, but only the scattering signal combinations whose two scattering signals arrive at two different BS are related to the localization of scatterers. Assuming that the number of scattering signal combinations related to the localization of scatterers is  $P$ , there are  $P$  potential scatterers corresponding to the  $P$  pairs scattering signal combination. Identifying with inequality Equation (5), we assume that the remaining are  $Q$  pairs scattering signal combinations. For urban or indoor environments, there are multiple scatterers usually, the  $Q$  pairs scattering signal combination may come from different scatterers, these scattering signal combinations should be divided into multiple groups according to their source scatterer.

For the division of scattering signal combinations according to source scatterer, firstly, we introduce the definition of adjacent combination.

**Definition 1.** (*adjacent combination*): if A scattering signal combination and B scattering signal combination have one same scattering signal, then A scattering signal combination is B scattering signal combination's adjacent combination, and the converse is true, that is, A scattering signal combination and B scattering signal combination is the mutual adjacent combination.

For instance, A scattering signal combination consists of scattering signal 1 and scattering signal 2, and B scattering signal combination consists of scattering signal 2 and scattering signal 4, the two combinations have the same scattering signal 2, so they are adjacent combinations.

When the number of BS is three, there are three scattering signals from a given scatterer to BSs at most, and the three scattering signals can form three pairs of scattering signal combinations, one is the other's adjacent combination. When the number of BS is four, there are four scattering signals at most from a given scatterer to BSs, and they can form six pairs of scattering signal combinations at most, accordingly. In the six pairs scattering signal combination, any scattering signal combination could find its adjacent combination in the rest other five pairs scattering signal combination. When the number of BS is more than four, among all scattering signal combinations of a given scatterer, any scattering signal combination could find its adjacent combination in the rest other scattering signal combinations, too. Moreover, the number of scattering signals from any scatterer should be less than or equal to the number of BS, therefore, if the number of scattering signals from one scatterer is larger than the number of BS in the result, corresponding data should be excluded as wrong data resulting from measurement error.

Based on the aforementioned characterization of the one-bounce scattering signal from the same scatterer, we can get Algorithm 1, which divides scattering signal combinations according to source scatterers, and each scattering signal combination set in Algorithm 1 corresponds to a source scatterer.

After dividing scattering signal combinations according to source scatterer, for each scattering signal combination set, we should further delete false scattering signal combinations resulting from measurement error, which may result in large errors in scatterer localization. To simplify the analysis, we take the deletion of false scattering signal combinations of one scattering signal combination set as an example of derivation in the following analysis, and the corresponding scatterer is referred to as target scatterer S.

**Algorithm 1:** Dividing scattering signal combinations according to the source scatterer**Input:** set  $C$  consisting of  $Q$  pairs scattering signal combination.**Output:** multiple scattering signal combination sets corresponding to multiple scatterers, respectively.**while** set  $C$  is not empty **do**

Construct a new empty scattering signal combination set.

Select a scattering signal combination from  $C$  randomly and insert it into the new set.Delete above scattering signal combination from  $C$ .**while** the number of scattering signal combination of set  $C$  decreases**for** each pair scattering signal combination of  $C$  **do****If** the new set has its adjacent combination

Insert it into new set.

Delete it in set  $C$ .**else**Remain it in set  $C$ .**end for****for** each scattering signal combination set **do**if the number of scattering signal > the number of BS  $M$ 

Delete this scattering signal combination set.

**end for**

Assuming that there are  $R$  pairs scattering signal combination in the scattering signal combination set corresponding to target scatterer  $S$ , the intersection points of  $R$  pairs scattering signal combination are all potential positions of scatterer  $S$ . Because of corresponding to the same scatterer  $S$ , the  $R$  potential positions of scatterer  $S$  should overlap with each other, but the result of estimating does not comply with this constraint for the reason of measurement error. Assuming that the coordinate estimate of potential scatterer  $S$  corresponding to scattering signal combination  $j$  is  $(\hat{x}_{s_j}, \hat{y}_{s_j}), j = 1, 2, \dots, R$ , the mean of  $R$  coordinate estimate of scatterer  $S$  is

$$\bar{x}_s = \frac{1}{R} \sum_{j=1}^R \hat{x}_{s_j}, \quad \bar{y}_s = \frac{1}{R} \sum_{j=1}^R \hat{y}_{s_j} \quad (6)$$

Thus, we can obtain the distance between  $(\hat{x}_{s_j}, \hat{y}_{s_j})$  and  $(\bar{x}_s, \bar{y}_s)$ , which is denoted by  $l_j$ . The mean of  $l_j$  for all potential positions  $(\hat{x}_{s_j}, \hat{y}_{s_j})$  is denoted by  $l_{mean}$ . The scattering signal combinations corresponding to the potential position  $(\hat{x}_{s_j}, \hat{y}_{s_j})$ , whose  $l_j$  is less than  $l_{mean}$ , are kept for the second step of the identification algorithm. Obviously, the number of scattering signal combinations  $R$  satisfies the following inequality

$$R \leq C_M^2, \quad (7)$$

and  $R = C_M^2$  holds only when  $M$  BSs all receive scattering signals from target scatterer  $S$ .

Up to now, we can get multiple scattering signal combination sets corresponding to multiple scatterers. The above procedure is the first step of the identification algorithm, which is also referred to as a one-step identification algorithm for short in the simulation analysis.

The aforementioned first step of the identification algorithm can be summarized as Algorithm 2.

**Algorithm 2:** First step of the identification algorithm

---

**Input:**  $N$  scattering signals from multiple scatterers to  $M$  BSs.  
**Output:** multiple scattering signal combination sets corresponding to multiple scatterers.  
Construct  $P$  pairs scattering signal combinations related to localization of scatterers from  $N$  scattering signals.  
**for** each scattering signal combination of  $P$  pairs scattering signal combination **do**  
    Compute Inequality (5).  
    **if** Inequality (5) holds  
        Corresponding scattering signal combination is kept.  
    **else**  
        Corresponding scattering signal combination is discarded.  
**end for**  
Divide the rest  $Q$  pairs scattering signal combination according to source scatterer.  
**for** each scattering signal combination set corresponding to a source scatterer **do**  
    Compute  $(\bar{x}_s, \bar{y}_s)$ .  
    **for** each scattering signal combination in set **do**  
        Compute  $l_j$ .  
    **end for**  
    Compute  $l_{mean}$ .  
    **for** each scattering signal combination in set **do**  
        **if**  $l_j < l_{mean}$   
            Corresponding scattering signal combination is kept.  
        **else**  
            Corresponding scattering signal combination is discarded.  
    **end for**  
**end for**

---

**3. Second Step of One-Bounce Scattering Signal Identification Algorithm**

After the first step of the identification algorithm, all scattering signals can be divided into multiple scattering signal combination sets, and each scattering signal combination set corresponds to a source scatterer, from which each scattering signal comes BS, respectively. The scattering signals of the scattering signal combination set can be used for the localization of the corresponding source scatterer. However, due to measurement error, some scattering signals may be mistakenly identified as scattering signals from the other scatterer, or some scattering signals' measurements of TOA or AOA may have large errors, these all would result in large MS localization error if these scattering signals are used for localization of scatterer and then scatterer is used as a virtual station for MS localization. In order to improve the MS localization accuracy, we have to delete these scattering signals by the second step of the identification algorithm. To simplify the analysis, we take the identification of scattering signals from one scatterer as an example of derivation in the following analysis, and this scatterer is referred to as target scatterer S.

**3.1. Localization of Scatterer**

Assuming there are  $W$  one-bounce scattering signals from target scatterer S to BSs after the first step of the identification algorithm. Clearly, the number of one-bounce scattering signal  $W$  is less than twice the number of scattering signal combinations of target scatterer S, because some scattering signal combinations have the same scattering signal. Accordingly, there are  $W$  BSs receiving one-bounce scattering signals from target scatterer S, assuming that the coordinate of scatterer S is  $(x_s, y_s)$ , the distance from the scatterer S to the  $i$ th BS is:

$$d_i = \sqrt{(x_i - x_s)^2 + (y_i - y_s)^2}, i = 1, 2, \dots, W \quad (8)$$

Suppose the distance between MS and scatterer S is  $d$ , then the TOA distance from  $i$ th BS to MS denoted by  $r_i$  satisfies  $r_i = d_i + d$ . With regarding 1st BS as a reference BS, the difference between  $r_i$  and  $r_1$  can be written as

$$r_{i,1} = r_i - r_1 = (d_i + d) - (d_1 + d) = d_i - d_1 = d_{i,1}, \tag{9}$$

where  $d_{i,1}$  is the difference between the distance from the scatterer S to the  $i$ th BS and that of 1st BS. Moreover, we can get

$$d_{i,1} = \sqrt{(x_i - x_s)^2 + (y_i - y_s)^2} - \sqrt{(x_1 - x_s)^2 + (y_1 - y_s)^2} \tag{10}$$

Linearizing Equation (10) and simplifying it gives

$$-x_{i,1}x_s - y_{i,1}y_s - d_{i,1}d_1 = \frac{d_{i,1}^2 - K_i + K_1}{2}, \tag{11}$$

where  $x_{i,1} = x_i - x_1$ ,  $y_{i,1} = y_i - y_1$  and  $K_i = x_i^2 + y_i^2$ .

When the number of BS, that is,  $W$  equals three, there are two BSs in addition to the 1st BS, from Equation (11) we can obtain two equations. Exploiting the two equations, the coordinate of scatterer S can be written in terms of  $d_1$

$$\begin{bmatrix} x_s \\ y_s \end{bmatrix} = - \begin{bmatrix} x_{2,1} & y_{2,1} \\ x_{3,1} & y_{3,1} \end{bmatrix}^{-1} \left\{ \begin{bmatrix} d_{2,1} \\ d_{3,1} \end{bmatrix} d_1 + \frac{1}{2} \begin{bmatrix} d_{2,1}^2 - K_2 + K_1 \\ d_{3,1}^2 - K_3 + K_1 \end{bmatrix} \right\}. \tag{12}$$

Putting Equation (12) into Equation (8) yields a quadratic in  $d_1$ , and then substituting the positive root of the quadratic in  $d_1$  into Equation (12),  $(x_s, y_s)$  can be obtained.

When  $W$  is more than three, Equation (11) yields more than two equations, combining Equation (8) gives more than three equations with three variables,  $x_s, y_s$  and  $d_1$ , the proper answer is the  $[x_s, y_s, d_1]$  that best fits these equations, which can be solved using two steps weighted least square (TSWLS) of [34].

Let  $z = [x_s, y_s, d_1]^T$ , and assuming that  $x_s, y_s$  and  $d_1$  are independent, we can obtain

$$z = \operatorname{argmin}\{(h - Gz)^T \varphi^{-1}(h - Gz)\} = (G^T \varphi^{-1} G)^{-1} G^T \varphi^{-1} h, \tag{13}$$

where  $\varphi = c^2 B Q B$ ,  $B = \operatorname{diag}\{d_2^0, d_3^0, \dots, d_N^0\}$ , the superscript  $\{*\}^0$  denotes the noise-free value,  $Q$  is covariance matrix of TDOA,  $c$  is signal propagation speed, and

$$G = - \begin{bmatrix} x_{2,1} & y_{2,1} & d_{2,1} \\ x_{3,1} & y_{3,1} & d_{3,1} \\ \vdots & \vdots & \vdots \\ x_{N,1} & y_{N,1} & d_{N,1} \end{bmatrix}, \quad h = \begin{bmatrix} d_{2,1}^2 - K_2 + K_1 \\ d_{3,1}^2 - K_3 + K_1 \\ \vdots \\ d_{N,1}^2 - K_N + K_1 \end{bmatrix}. \tag{14}$$

When the scatterer is far away from BSs, Equation (13) can be approximated as

$$z \approx (G^T Q^{-1} G)^{-1} G^T Q^{-1} h. \tag{15}$$

When the scatterer is close to BSs,  $z$  can be solved with Equation (13) on the basis of the initial solution provided by Equation (15).

Furthermore, remove the assumption that  $x_s, y_s$  and  $d_1$  are independent, let

$$z_1 = x_s^0 + e_1, \quad z_2 = y_s^0 + e_2, \quad z_3 = d_1^0 + e_3, \tag{16}$$

where  $e_1, e_2$  and  $e_3$  are estimation errors of  $z$ , then the vector  $\varphi'$  denoting inaccuracies in  $z$  is found to be

$$\varphi' = h' - G' z'^0, \tag{17}$$

where

$$h' = \begin{bmatrix} (z_1 - x_1)^2 \\ (z_2 - y_1)^2 \\ z_3 \end{bmatrix}, G' = \begin{bmatrix} 1 & 0 \\ 0 & 1 \\ 1 & 1 \end{bmatrix}, z' = \begin{bmatrix} (x_s - x_1)^2 \\ (y_s - y_1)^2 \end{bmatrix}. \tag{18}$$

The covariance matrix of  $\varphi'$  is

$$\varphi' = E[\varphi' \varphi'^T] = 4B' \text{cov}(z) B', \tag{19}$$

where  $B' = \text{diag}\{x^0 - x_1, y^0 - y_1, r_1^0\}$ , thus the weighted least square (WLS) estimate of  $z'$  is

$$z' = (G'^T \varphi'^{-1} G')^{-1} G'^T \varphi'^{-1} h'. \tag{20}$$

Then after some operations, the final position estimate of scatterer S is obtained from  $z'$  as

$$\begin{bmatrix} x_s \\ y_s \end{bmatrix} = \sqrt{z'} + \begin{bmatrix} x_1 \\ y_1 \end{bmatrix} \text{ or } \begin{bmatrix} x_s \\ y_s \end{bmatrix} = -\sqrt{z'} + \begin{bmatrix} x_1 \\ y_1 \end{bmatrix} \tag{21}$$

The proper solution selected is the one that follows the prior information about the scatterer.

### 3.2. Identification of Scattering Signal Based on AOA

For the  $W$  one-bounce scattering signals of scatterer S,  $3 \sim W$  signals are randomly selected from  $W$  signals as a combination, so there are  $sum = C_W^3 + C_W^4 + \dots + C_W^W$  combinations. For each combination, the coordinate of the scatterer  $(\hat{x}_s, \hat{y}_s)$  can be estimated by Equation (12) or Equation (21). Thus, for the scattering signal from target scatterer S to  $i$ th BS in combination  $s$ , its estimate of AOA denoted by  $\theta_i$ , can be computed as follows

$$\theta_i = \arctan\left(\frac{y_i - \hat{y}_s}{x_i - \hat{x}_s}\right) \tag{22}$$

Suppose that the corresponding measurement of scattering signal from target scatterer S to  $i$ th BS is  $\alpha_i$ , the scattering signal should satisfy  $\alpha_i = \theta_i$  under the condition of absence of measurement error. However, due to the presence of measurement error,  $\alpha_i = \theta_i$  is not guaranteed. For each combination of scattering signals, the sum of absolute values of the difference between  $\theta_i$  and  $\alpha_i$  can be expressed as

$$DF = \sum_i |\theta_i - \alpha_i| \tag{23}$$

The scattering signals in the combination that minimizes  $DF$  are selected to be the one-bounce scattering signals from the same scatterer S, which can be used for the localization of scatterer S.

Based on the aforementioned derivation, the second step of the identification algorithm for a scatterer can be summarized as Algorithm 3.

The complete identification algorithm including the first and second steps is demonstrated in Figure 2 and is referred to as the two-step identification algorithm for short in the simulation analysis.

**Algorithm 3:** Second step of identification algorithm for a scatterer**Input:**  $W$  scattering signals from scatterers  $S$  to  $W$  BSs.**Output:** scattering signals used for localization of scatterer  $S$ .3~ $W$  scattering signals are randomly selected to form *sum* scattering signal combinations.**for** each combination of the *sum* scattering signal combinations **do**    Compute the coordinate of the scatterer  $(x_s, y_s)$ .    **for** each scattering signal of combination **do**        Compute  $|\theta_i - \alpha_i|$ .    **end for**    Compute  $\sum_i |\theta_i - \alpha_i|$ .**end for**Select the scattering signals in the combination that minimize  $\sum_i |\theta_i - \alpha_i|$ .**4. Virtual Station Localization Algorithm Based on Scattering Signal Identification**

On the basis of the identification of a one-bounce scattering signal from the same scatterer, we can easily locate scatterers. Once the scatterers are located, the distance between the scatterer and BS can be computed, and then the distance between the scatterer and MS can be computed based on the TOA distance from MS to BS. Regarding scatterers as virtual stations, MS can be located with the existing LOS localization algorithm.

Misidentification of scattering signal will lead to significant scatterer localization error, which may result in a much larger MS localization error. To eliminate MS localization error resulting from the misidentification of scattering signal, in the localization procedure of MS, we adopt four scatterers as four virtual stations, in GNSS-denied urban or indoor environments, four or more scatterers can be achieved. The four virtual stations are divided into four virtual station combinations, each virtual station combination has three virtual stations for LOS localization of MS. Consequently, there are four estimated positions of MS. As long as the probability of scattering signal misidentification of one scatterer is small enough, the probability of scattering signal misidentification of two scatterers will be even smaller. For instance, if the probability of scattering signal misidentification of a scatterer is less than 10%, then the corresponding probability of two scatterers will be less than  $10\% * 10\% = 1\%$ , such that we can consider that there is at most one scatterer whose scattering signal is misidentified in the four scatterers.

Furthermore, due to there being at most one scatterer whose scattering signal is misidentified in the four scatterers, there is at most one scatterer that has a significant localization error in the four scatterers. Therefore, among the four virtual station combinations with every three virtual stations, at most one virtual station combination has a scatterer that has a significant localization error. So, we can consider that there is at most one virtual station combination that has a significant MS localization error, which results from one of its three scatterer's scattering signals being misidentified. Hence, in the four estimated positions of MS, corresponding to the four virtual station combinations, at most one estimated position is far away from the MS. The estimated position, which is relatively far away from the other three positions, should be discarded as an outlier, and the mean of the rest three positions is adopted as the estimated position of MS ultimately. The discarding of outliers eliminates the error resulting from scattering signal misidentification, this kind of error may lead to huge errors in the MS localization procedure. Averaging the other three estimated positions of MS helps further reduce MS localization errors. The virtual station localization algorithm can be summarized as algorithm 4.

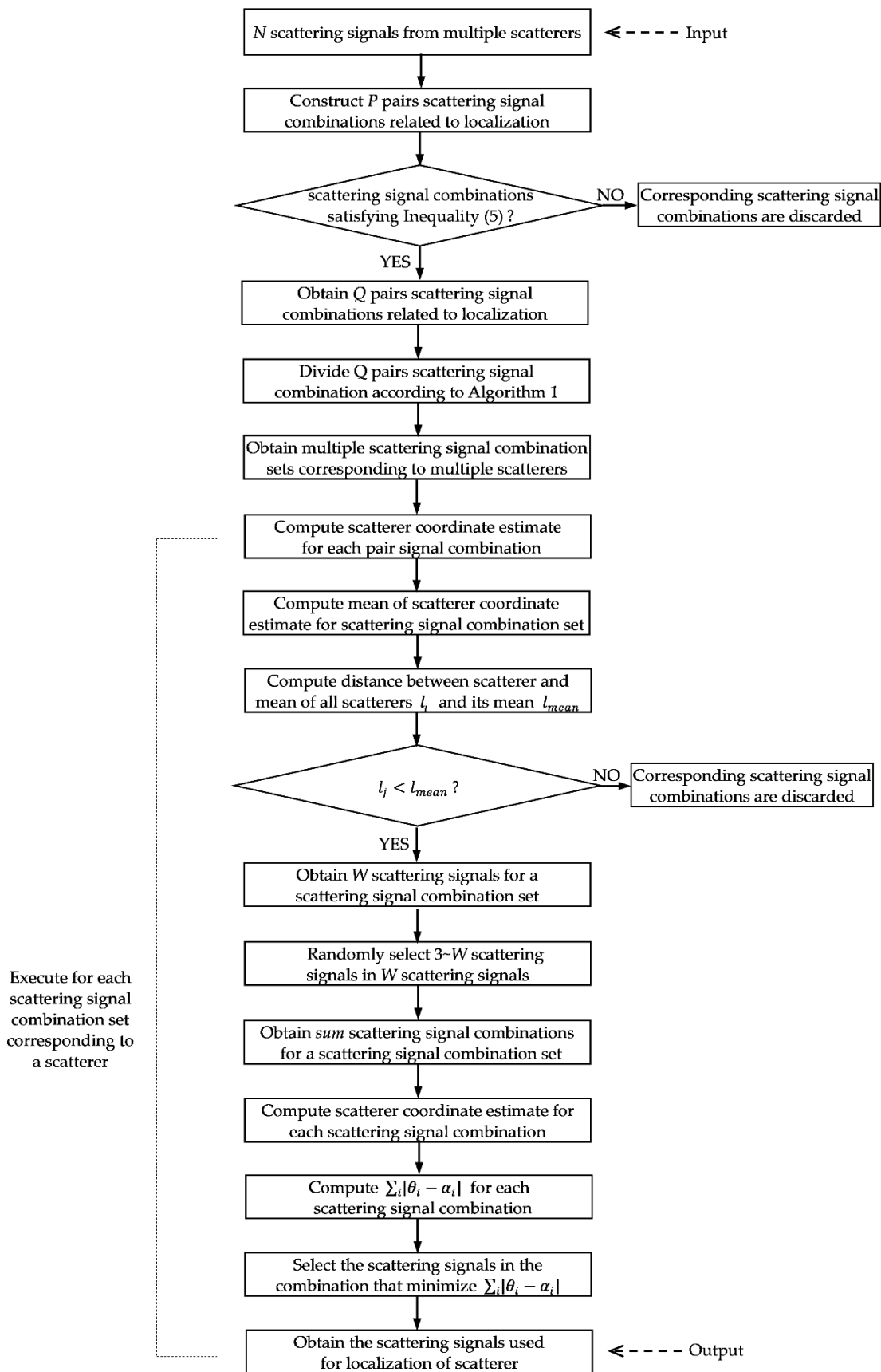


Figure 2. Flow chart of two-step one-bounce scattering signal identification algorithm used for localization of scatterer.

**Algorithm 4:** Virtual station localization algorithm**Input:** four groups scattering signal corresponding to four scatterers.**Output:** localization of MS.**for** each group scattering signal **do**

Estimate position of scatterer.

**end for**

Create four virtual station combinations with every three scatterers.

**for** each virtual station combination **do**

Estimate position of MS with LOS algorithm.

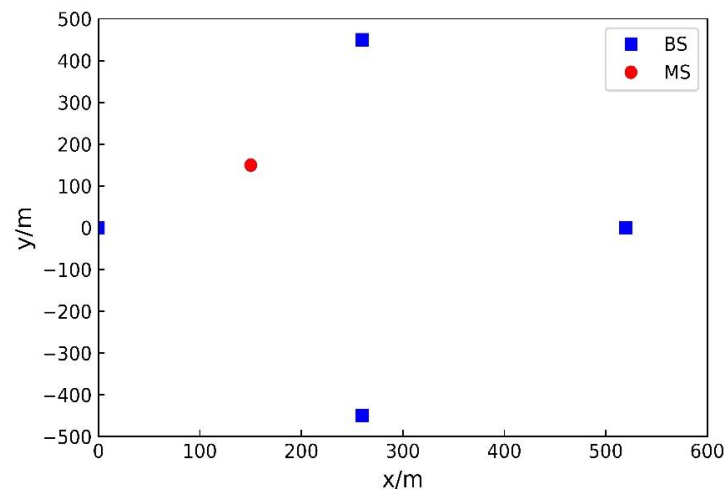
**end for**

Discard the outlier in four estimated positions of MS.

Select the mean of the rest three positions as MS position ultimately.

**5. Simulation and Analysis**

Simulations are carried out to evaluate the performance of the proposed algorithm. The following scenario is considered for data generation. As shown in Figure 3, cell radius  $R$  is assumed to be 300 m, four BSs are located at BS1  $(0, 0)$ , BS2  $(\sqrt{3}R, 0)$ , BS3  $(\sqrt{3}R/2, 3R/2)$  and BS4  $(\sqrt{3}R/2, -3R/2)$ , respectively. The MS is located at  $(R/2, R/2)$ . Four scatterers are randomly distributed around the MS, which satisfies the ring-of-scatterer (ROS) model or disk-of-scatterer (DOS) model. Each of the data in the below figures is calculated from 1000 independent trials, the measurement error of distance of TOA and AOA satisfies zero-mean Gaussian distribution, the unit of distance is meter (m), and the unit of AOA is degree ( $^\circ$ ). The identification performance is evaluated using the identification rate ( $P_{IE}$ ), defined by  $P_{IE} = N_C/N_T$ , with  $N_T$  being the number of all scattering signal combinations and  $N_C$  being the number of scattering signal combinations that are identified correctly.

**Figure 3.** Localization of geometry.**5.1. Performance Analysis of Identification Algorithm**

First, we discuss how to choose the proper identification threshold in the first step of the one-bounce scattering signal identification algorithm. Assuming scatterers are generated by the ROS model, the scattering radius is 50 m and the error of TOA satisfies  $N(0, 1^2)$  and the error of AOA satisfies  $N(0, 0.5^2)$ . For the first step of the proposed algorithm, false alarm probability and alarm dismissal probability versus identification threshold are shown in Figure 4. With the increasing threshold value, false alarm probability increases but alarm dismissal probability decreases, and when the threshold value is 35 m, the sum of false alarm probability and alarm dismissal probability attains a minimum value of 27.51%, therefore, we adopt 35 m as the threshold value in the following simulations.

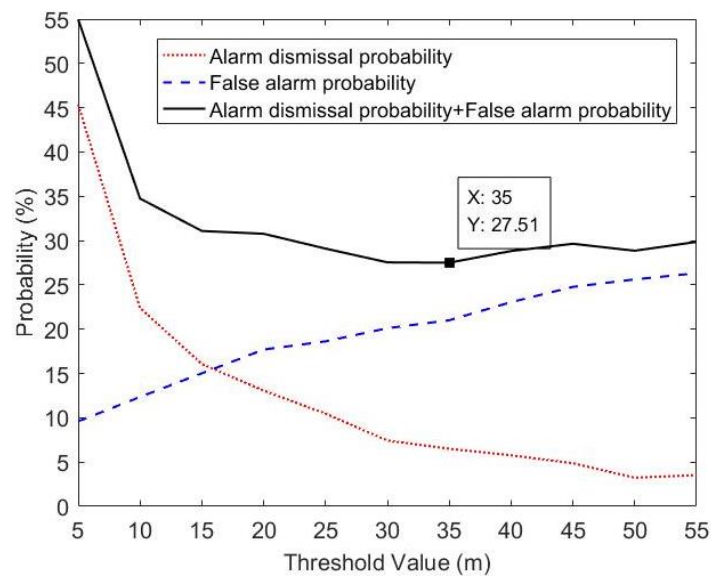


Figure 4. Effect of identification threshold on false alarm probability and alarm dismissal probability.

The  $P_{IE}$  versus scattering radius comparison is presented in Figure 5. The scattering radius is 10 m, 20 m, 30 m, 40 m, 50 m, 60 m and 70 m, respectively. The scatterers are generated following the ROS model or DOS model. The error of TOA satisfies  $N(0, 1^2)$ , and that of AOA satisfies  $N(0, 0.5^2)$ . It can be observed that with the increasing scattering radius from 10 m to 70 m identification algorithm’s performance is improved, and  $P_{IE}$  of the two-step algorithm, up to 95%, the probability of scattering signal misidentification of a scatterer is just 5%, which is small enough. The two-step algorithm outperforms the one-step algorithm indicating that the second step is necessary. As Figure 5 shows, for the same scattering radius, the  $P_{IE}$  under the condition of ROS mode is superior to that of the DOS model, this is because the distance between two scatterers under the condition of the ROS model is larger than that of the DOS model for the same scattering radius, which is in favor of distinguishing scattering signals.

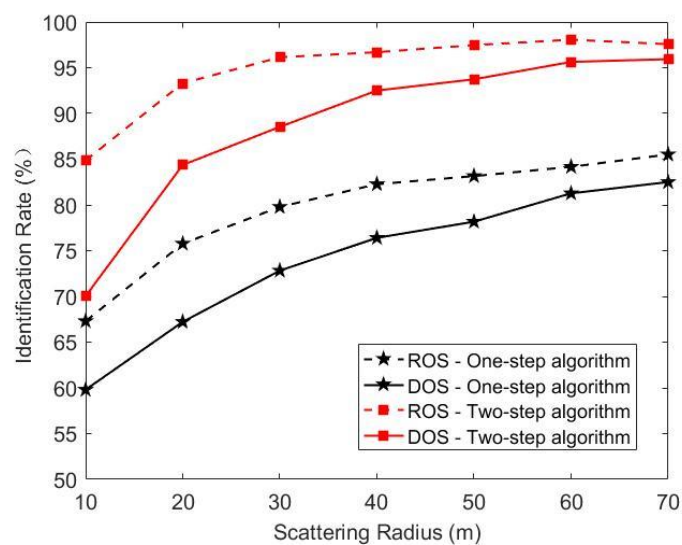


Figure 5.  $P_{IE}$  versus scattering radius.

We vary the standard deviations of TOA error to evaluate the algorithm’s performance. The scatterers are generated following the ROS model or DOS model, respectively, scattering radius is 50 m. The error of TOA satisfies  $N(0, \delta_T^2)$ ,  $\delta_T$  is 1 m, 2 m, 3 m, 4 m and 5 m, respectively, and the error of AOA satisfies  $N(0, 0.5^2)$ . As depicted in Figure 6, the growth

of the standard deviation of the TOA error has little effect on the one-step algorithm, whereas, with the growth of the standard deviation of the TOA error, the performance of the two-step algorithm deteriorates. This is because, in the identification procedure, the second step of the two-step algorithm adopts the measurements of TOA to estimate the coordinates of the scatterer first, and then on this basis, adopts the scattering signals combination that minimizes the sum of absolute values of the difference between the estimates and measurements of AOA, this procedure is sensitive to the variation of scatterer coordinate, thus, with the increasing standard deviation of the TOA, the  $P_{IE}$  performance of the two-step algorithm deteriorates. Similar to Figure 5, the  $P_{IE}$  performance of the two-step is superior to that of the one-step algorithm, and the  $P_{IE}$  performance under the condition of the ROS model is better than that of the DOS model.

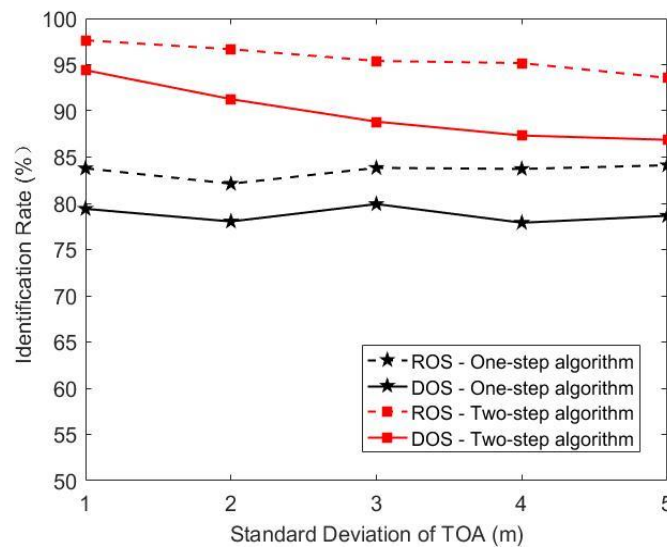


Figure 6.  $P_{IE}$  versus  $\delta_T$ .

The  $P_{IE}$  versus AOA error comparison is presented in Figure 7. The scatterers are generated following the ROS model or DOS model, respectively, scattering radius is 50 m. The error of AOA satisfies  $N(0, \delta_A^2)$ ,  $\delta_A$  is  $0.2^0$ ,  $0.4^0$ ,  $0.6^0$ ,  $0.8^0$ , and  $1^0$ , respectively, and the error of TOA satisfies  $N(0, 1^2)$ . It can be seen from Figure 7, similar to Figure 6, the  $P_{IE}$  performance of the one-step algorithm is not sensitive to the variation of the standard deviation of AOA error, but the  $P_{IE}$  performance of the two-step algorithm deteriorates with the growing standard deviation of AOA error. The reason is similar to that of Figure 6 because the second step of the two-step algorithm adopts the scattering signals combination that minimizes the sum of absolute values of the difference between estimates and measurements of AOA, which result in performance deterioration with the increasing of the standard deviation of the TOA. Similar to Figures 5 and 6, the performance of the two-step algorithm is superior to that of the one-step algorithm, and the performance under the condition of the ROS model outperforms that of the DOS model.

### 5.2. Performance Analysis of Hybrid TOA/AOA Virtual Station Localization Algorithm

MS localization accuracy of the proposed algorithm is compared with the other hybrid TOA/AOA algorithms, improved grid search algorithm (IGSA) [35], hybrid TOA/AOA algorithm (HTA) [36] and new TOA/AOA constrained algorithm (NTA-CA) [37], with cumulative distribution function (CDF) curve of MS localization error. The error of TOA and AOA satisfies  $N(0, 1^2)$  and  $N(0, 0.5^2)$ , respectively. As shown in Figure 8, for the case of the DOS model, at a probability of 90%, the localization error of the proposed algorithm is about 5 m, whereas that of IGSA, HTA and NTA-CA is about 30 m, 45 m and 60 m for the same probability, respectively. Clearly, the proposed algorithm outperforms all other

hybrid TOA/AOA algorithms greatly. The case of the ROS model is similar to that of the DOS model as shown in Figure 9.

In the proposed localization algorithm, the MS localization is based on the scatterer localization, the localization error of the scatterer will propagate to the procedure of MS localization. The MS localization error can be divided into two parts: the localization error derived from the scatterer localization stage and the localization error derived from the MS localization stage. MS localization error should be greater than that of the scatterer, this conclusion roughly agrees with Figures 8 and 9. Moreover, it can be observed that with the increasing localization error, the CDF curve of MS gradually approaches and eventually almost coincides with that of the scatterer, which demonstrates that, as the localization error increases, the localization error derived from the MS localization stage is almost gradually eliminated by the averaging of the rest three estimated positions of MS in MS localization stage.

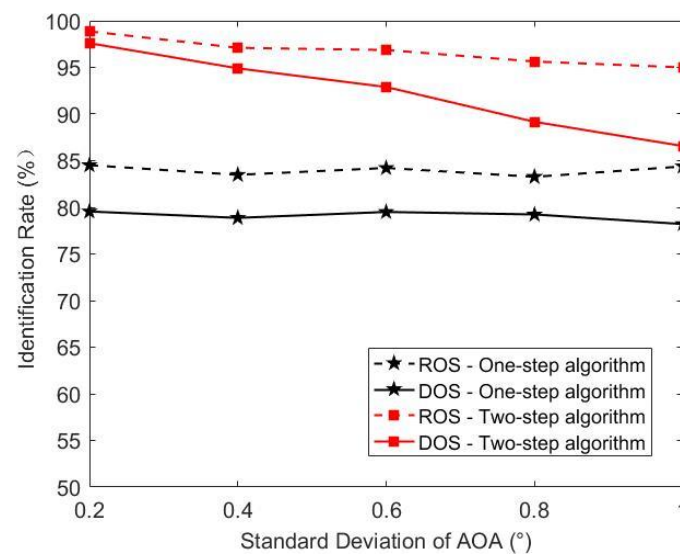


Figure 7.  $P_{IE}$  versus  $\delta_A$ .

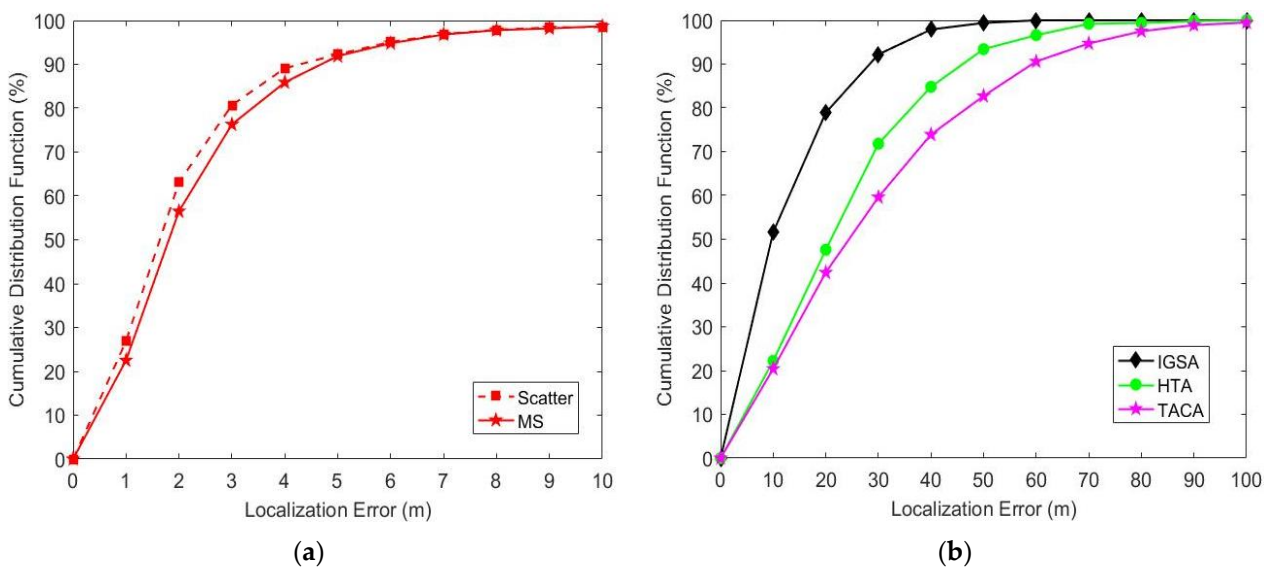
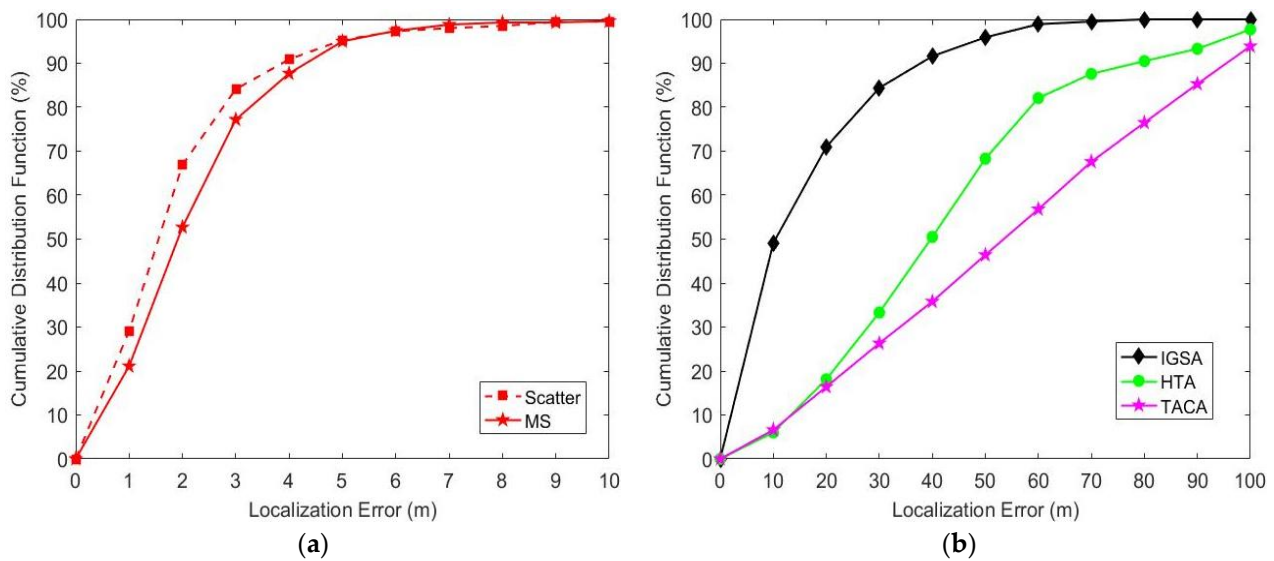


Figure 8. Localization error CDFs curve for DOS model. (a) The curve of proposed algorithm; (b) The curve of IGSA, HTA and NTA-CA.



**Figure 9.** Localization error CDFs curve for ROS model. (a) The curve of proposed algorithm; (b) The curve of IGSA, HTA and NTA-CA.

## 6. Conclusions and Future Research

GNSS provides high-accuracy real-time localization services in outdoor open-sky environments, but in GNSS-denied urban or indoor environments, accurate localization is still an unsolved problem due to the unavailability or degradation of GNSS signals. For localization technologies based on mobile communication networks or other wireless technologies, obstructions between the source and receivers will result in NLOS propagation, which significantly degrades the localization performance. Accurate localization in the presence of NLOS propagation has attracted considerable research focus due to it is the premise of many technologies and applications. In this paper, for GNSS-denied urban or indoor NLOS environments and localization technologies based on mobile communication networks or other wireless technologies, a hybrid TOA/AOA virtual station localization algorithm based on scattering signal identification is proposed. Without requiring any assumption or prior knowledge about MS, scatterer and BS, and only based on the geometric relationship of MS, scatterer and BS, a two-step one-bounce scattering signal identification algorithm is proposed. Simulation results demonstrate that the identification rate of the one-bounce scattering signal from the same scatterer can up to 95%, which provide a solid foundation for the following virtual station localization algorithm. On this basis, regarding four scatterers as virtual stations, we propose a novel virtual station localization algorithm, which almost eliminates localization error resulting from scattering signal misidentification. Simulation results show that the MS localization performance of proposed algorithm outperforms the state-of-the-art hybrid TOA/AOA localization algorithms, as far as we know. In this paper, we explore false alarm probability and alarm dismissal probability versus identification threshold by simulation, and choose the identification threshold  $D$ , which minimizes the sum of false alarm probability and alarm dismissal probability, for our simulation scenario. For future work, the specific relationship between identification threshold  $D$  and false alarm probability will be investigated.

**Author Contributions:** This paper is a collaborative work by all the authors. Conceptualization and methodology, R.L. and L.Y.; analysis, R.L., L.Y.; writing—original draft preparation, R.L. and L.Y.; writing—review and editing, Y.K. and P.D. All authors have read and agreed to the published version of the manuscript.

**Funding:** This research was funded by National Nature Science Foundation of China [No.61871332], Sichuan Science and Technology Program [grant numbers:2021YFG0169], [grant numbers: 2022YFG0190] and Chengdu Normal University Science and Technology Project [no. 111/111159001].

**Institutional Review Board Statement:** Not applicable.

**Informed Consent Statement:** Not applicable.

**Data Availability Statement:** The data used to support the findings of this study are available from the corresponding author upon request.

**Acknowledgments:** We would like to thank the reviewers for their valuable comments and pointing out possible further research topics.

**Conflicts of Interest:** The authors declare no conflict of interest.

## References

1. Beck, A.; Stoica, P.; Li, J. Exact and approximate solutions of source localization problems. *IEEE Trans. Signal Process.* **2008**, *56*, 1770–1778. [[CrossRef](#)]
2. Zou, Y.; Wan, Q. Asynchronous time-of-arrival-based source localization with sensor position uncertainties. *IEEE Commun. Lett.* **2016**, *20*, 1860–1863. [[CrossRef](#)]
3. Zou, Y.; Fan, J.; Wu, L.; Liu, H. Fixed Point Iteration Based Algorithm for Asynchronous TOA-Based Source Localization. *Sensors* **2022**, *22*, 6871. [[CrossRef](#)] [[PubMed](#)]
4. Nguyen, N.H.; Dogancay, K. Optimal geometry analysis for multistatic TOA localization. *IEEE Trans. Signal Process.* **2016**, *64*, 4180–4193. [[CrossRef](#)]
5. Abu-Shaban, Z.; Zhou, X.; Abhayapala, T.D. A novel TOA-based mobile localization technique under mixed LOS/NLOS conditions for cellular networks. *IEEE Trans. Veh. Technol.* **2016**, *65*, 8841–8853. [[CrossRef](#)]
6. Zou, Y.; Liu, H.; Xie, W.; Wan, Q. Semidefinite programming methods for alleviating sensor position error in TDOA localization. *IEEE Access* **2017**, *5*, 23111–23120. [[CrossRef](#)]
7. Qiao, T.; Redfield, S.; Abbasi, A.; Su, Z.; Liu, H. Robust coarse position estimation for TDOA localization. *IEEE Wirel. Commun. Lett.* **2013**, *2*, 623–626. [[CrossRef](#)]
8. Altaf Khattak, S.B.; Fawad; Nasralla, M.M.; Esmail, M.A.; Mostafa, H.; Jia, M. WLAN RSS-Based Fingerprinting for Indoor Localization: A Machine Learning Inspired Bag-of-Features Approach. *Sensors* **2022**, *22*, 5236. [[CrossRef](#)]
9. Wang, G.; Yang, K. A new approach to sensor node localization using rss measurements in wireless sensor networks. *IEEE Trans. Wirel. Commun.* **2011**, *10*, 1389–1395. [[CrossRef](#)]
10. Li, C.; Zhen, J.; Chang, K.; Xu, A.; Zhu, H.; Wu, J. An Indoor Positioning and Tracking Algorithm Based on Angle-of-Arrival Using a Dual-Channel Array Antenna. *Remote Sens.* **2021**, *13*, 4301. [[CrossRef](#)]
11. Pan, T.; Chang, J.C.; Shen, C.C. Hybrid TOA/AOA measurements based on the Wiener estimator for cellular network. In Proceedings of the IEEE 12th International Conference on Networking, Sensing and Control, Taipei, Taiwan, 9–11 April 2015.
12. Zekavat, S.A.; Buehrer, R.M. *Handbook of Position Location: Theory, Practice and Advances*, 2nd ed.; Wiley: Hoboken, NJ, USA, 2019.
13. Chan, Y.T.; Tsui, W.Y.; So, H.C.; Ching, P.-C. Time-of-arrival based localization under NLOS conditions. *IEEE Trans. Veh. Technol.* **2006**, *55*, 17–24. [[CrossRef](#)]
14. Chen, Z.; Xu, A.; Sui, X.; Wang, C.; Wang, S.; Gao, J.; Shi, Z. Improved-UWB/LiDAR-SLAM Tightly Coupled Positioning System with NLOS Identification Using a LiDAR Point Cloud in GNSS-Denied Environments. *Remote Sens.* **2022**, *14*, 1380. [[CrossRef](#)]
15. Cong, L.; Zhuang, W. Nonline-of-sight error mitigation in mobile location. *IEEE Trans. Wirel. Commun.* **2005**, *4*, 560–573. [[CrossRef](#)]
16. Yu, X.; Wu, C.; Cheng, L. Indoor localization algorithm for TDOA measurement in NLOS environments. *IEICE Trans. Fundam. Electron. Commun. Comput. Sci.* **2014**, *E97.A*, 1149–1152. [[CrossRef](#)]
17. Yan, L.; Lu, Y.; Zhang, Y. An improved NLOS identification and mitigation approach for target tracking in wireless sensor networks. *IEEE Access* **2017**, *5*, 2798–2807. [[CrossRef](#)]
18. Luo, H.; Liu, S.; Liu, X. NLoS mitigation in ToA localization based on spatial correlation iter and iterative minimum residual. *China Commun.* **2012**, *9*, 13–19.
19. Wang, W.; Zhang, Y.; Tian, L. TOA-based NLOS error mitigation algorithm for 3D indoor localization. *China Commun.* **2020**, *17*, 63–72. [[CrossRef](#)]
20. Li, S.; Hedley, M.; Collings, I.B.; Humphrey, D. TDOA-based localization for semi-static targets in NLOS environments. *IEEE Wirel. Commun. Lett.* **2015**, *4*, 513–516. [[CrossRef](#)]
21. Yang, M.; Jackson, D.R.; Chen, J.; Xiong, Z.; Williams, J.T. A TDOA localization method for Nonline-of-Sight scenarios. *IEEE Trans. Antennas Propag.* **2019**, *67*, 2666–2676. [[CrossRef](#)]
22. Wu, S.; Zhang, S.; Huang, D. A TOA-based localization algorithm with simultaneous NLOS mitigation and synchronization error elimination. *IEEE Sens. Lett.* **2019**, *3*, 1–4. [[CrossRef](#)]
23. Han, K.; Shi, L.; Deng, Z.; Fu, X.; Liu, Y. Indoor NLOS positioning system based on enhanced CSI feature with intrusion adaptability. *Sensors* **2020**, *20*, 1211. [[CrossRef](#)] [[PubMed](#)]
24. Cao, B.; Wang, S.; Ge, S.; Ma, X.; Liu, W. A novel mobile target localization approach for complicate underground environment in mixed LOS/NLOS scenarios. *IEEE Access* **2020**, *8*, 96347–96362. [[CrossRef](#)]

25. Chen, Z.; Xu, A.; Sui, X.; Hao, Y.; Zhang, C.; Shi, Z. NLOS Identification- and Correction-Focused Fusion of UWB and LiDAR-SLAM Based on Factor Graph Optimization for High-Precision Positioning with Reduced Drift. *Remote Sens.* **2022**, *14*, 4258. [[CrossRef](#)]
26. Zhaounia, M.; Landolsi, M.A.; Bouallegue, R. A novel scattering distance-based mobile positioning algorithm. In Proceedings of the Global Information Infrastructure Symposium, Hammamet, Tunisia, 23–26 June 2009.
27. Yang, T.C.; Jin, L. Single station location method in NLOS environment: The circle fitting algorithm. *Sci. China Inf. Sci.* **2011**, *54*, 381–385. [[CrossRef](#)]
28. Liu, D.; Liu, K.; Ma, Y.; Yu, J. Joint TOA and DOA localization in indoor environment using virtual stations. *IEEE Commun. Lett.* **2014**, *18*, 1423–1426. [[CrossRef](#)]
29. Liu, D.; Wang, Y.; He, P.; Zhai, Y.; Wang, H. TOA localization for multipath and NLOS environment with virtual station. *EURASIP J. Wirel. Commun. Netw.* **2017**, *2017*, 104. [[CrossRef](#)]
30. Zhang, R.; Xia, W.; Yan, F.; Shen, L. A single-site positioning method based on TOA and DOA estimation using virtual stations in NLOS environment. *China Commun.* **2019**, *16*, 146–159.
31. Deng, Z.; Zheng, X.; Zhang, C.; Wang, H.; Yin, L.; Liu, W. A TDOA and PDR Fusion Method for 5G Indoor Localization based on Virtual Base Stations in Unknown Areas. *IEEE Access* **2020**, *8*, 225123–225133. [[CrossRef](#)]
32. Kuipers, B.W.M.; Mackowiak, M.; Correia, L.M. Understanding geometrically based multiple bounce channel models. In Proceedings of the 2nd European Conference on Antennas and Propagation (EuCAP 2007), Edinburgh, UK, 11–16 November 2007.
33. Liang, J.H.; He, J.; Yu, W.X.; Truong, T.K. Single-Site 3-D Positioning in Multipath Environments Using DOA-Delay Measurements. *IEEE Commun. Lett.* **2021**, *25*, 2559–2563. [[CrossRef](#)]
34. Chan, Y.T.; Ho, K.C. A simple and efficient estimator for hyperbolic location. *IEEE Trans. Signal Process.* **1994**, *42*, 1905–1915. [[CrossRef](#)]
35. Lu, Y.; Xiang, Z. Study on hybrid location algorithm based on single-bounced circle model. *Comput. Meas. Control* **2016**, *24*, 203–205.
36. Venkatraman, S.; Caffery, J. Hybrid TOA/AOA techniques for mobile location in non-line-of-sight environments. In Proceedings of the Wireless Communications and Networking Conference, Atlanta, GA, USA, 21–25 March 2004.
37. Wu, S.X.; Xu, D.Y.; Wang, H.G. Joint TOA/AOA Location Algorithms with Two BSs in Circular Scattering Environments. *WSEAS Trans. Commun.* **2015**, *14*, 235–240.